An Analysis of Eddy Current and Lorentz Force of Thin Plates under Moving Magnets

M. Tsuchimoto and K. Miya
Nuclear Engineering Research Laboratory
Faculty of Engineering, University of Tokyo
Tokai, Ibaraki 319-11, Japan

A. Yamashita
Railway Technical Research Institute
Kokubunji, Tokyo185, Japan

M. Hashimoto
Department of Electrical Engineering
University of Industrial Technology
Sagamihara, Kanagawa 229, Japan

Abstract **- Eddy current and Lorentz force induced into metallic thin plates by the passage of a high speed magnetic levitation vehicle are analyzed by using the current vector potential method (T-method) and the integral equation method (IEM). Kirchhoff's current law is imposed on the analysis of a branch structure, and flux penetrating a hole is considered to solve a multiply connected problem. Total eddy current and total Lorentz force are analyzed for several small thin plates.**

INTRODUCTION

A test line of a high speed magnetic levitation vehicle is now under construction in Japan. The vehicle has pairs of 700 kAT superconducting magnets and its maximum speed is about 500 km/h [1, 2]. By the passage of the vehicle, complex, strong and fluctuating magnetic field is applied and eddy current is induced in metallic guide way structures. Estimations of Lorentz force are important for evaluations of magnetic drag force, structural integrity and energy loss of the system [1-6]. In the present paper, eddy current and Lorentz force induced in metallic thin plates are analyzed by using the current vector potential method (T-method) [7-9] and the integral equation method (IEM) [10, 11]. Advantages of the T-method used here are : (1) only one variable, (2) no variables in space and (3) an easy treatment of the external current and field. When the eddy current distribution is assumed constant through the thickness of a plate, the analysis is reduced to a scalar problem. Kirchhoff's current law is imposed to the analysis of a branch structure and the flux penetrating a hole is considered to solve a multiply connected problem. In the IEM, first derivatives, which correspond to eddy current in the T-method, are obtained with high accuracy. The total eddy current and the total Lorentz force are analyzed for several small thin plates and it is shown that the T-method and the IEM are useful to analyze the problem.

FORMULATION

When the eddy current distribution is assumed constant through the thickness of the plate, the governing equation of the T-method is obtained from Maxwell equations and Biot-Savart's law [7-9] :

$$\frac{1}{\sigma}\nabla^2 T - \mu_0(\dot{T}+\frac{1}{4\pi}\mathbf{n}\bullet\int \dot{T}\nabla'\frac{1}{R}dS) = \mathbf{n}\bullet\dot{\mathbf{B}}_0 , \qquad (1)$$

where T is a normal component of the current vector potential **T** defined as follows [7-9] :

$$\nabla\times\mathbf{T} = \mathbf{J}_e . \qquad (2)$$

In above equation, $\mu_0, \sigma, \mathbf{J}_e, \mathbf{B}_0$, R are magnetic permeability in air, electric conductivity, eddy current density, applied magnetic field for the plate and a distance between a source point and a field point, respectively. **n** is a unit normal vector on surfaces of the plate, and " $\bullet$ " and " ' " indicate time derivative and an operation with regard to the source point, respectively. In the thin plate analysis, the Coulomb gauge is satisfied automatically and the boundary condition becomes T=constant on the edge of the plate. When a fundamental solution ϕ^* of the Laplace operator is used as a weighting function in a weighted residual procedure, the following integral equation is obtained [11] :

$$C_iT_i + \fint_\Gamma T\frac{\partial\phi^*}{\partial n}d\Gamma - \fint_\Gamma \phi^*\frac{\partial T}{\partial n}d\Gamma +$$
$$\int_\Omega \phi^*\mu_0\sigma(\dot{T}+\frac{1}{4\pi}\mathbf{n}\bullet\int \dot{T}\frac{\partial}{\partial n'}\frac{1}{R}dS)d\Omega = -\int_\Omega \phi^*\sigma\mathbf{n}\bullet\dot{\mathbf{B}}_0 d\Omega , \qquad (3)$$

where Γ is the boundary of the domain Ω, and $\fint$ denotes Cauchy principal value integration. The coefficient C_i at the field point is evaluated as follows for the sufficiently smooth boundary Γ :

$$C_i=0 \text{ if } i\notin\Gamma+\Omega,\quad C_i=1/2 \text{ if } i\in\Gamma,\quad C_i=1 \text{ if } i\in\Omega. \qquad (4)$$

Then the following matrix equations are obtained for the boundary and the domain respectively :

$$[\mathbf{P}]\{e_\Gamma\} = [\mathbf{Q}]\{\bar{e}_\Gamma\} + [\mathbf{A}]\{T_\Omega\} + \{a\} , \qquad (5)$$

$$\{T_i\} = [\mathbf{E}]\{e_\Gamma\} + [\mathbf{F}]\{\bar{e}_\Gamma\} + [\mathbf{K}]\{T_\Omega\} + \{k\} , \qquad (6)$$

Manuscript received July 7, 1991.

where $\{e_\Gamma\}$ is an unknown value on the boundary and $\{\bar{e}_\Gamma\}$ is the boundary condition. In the IEM analysis, $\{T_\Omega\}$ in (5) is also an unknown, and (5) is combined to (6) to solve the problem [11]. Since the matrix [P] in (5) is a square matrix, there is an inverse matrix :

$$\{e_\Gamma\} = [\mathbf{P}]^{-1}([\mathbf{Q}]\{\bar{e}_\Gamma\} + [\mathbf{A}]\{T_\Omega\} + \{a\}) . \qquad (7)$$

Equation (7) is substituted for (6), and both position and number of $\{T_i\}$ are matched with those of $\{T_\Omega\}$:

$$\{T_\Omega\} - ([\mathbf{E}][\mathbf{P}]^{-1}[\mathbf{A}] + [\mathbf{K}])\{\dot{T}_\Omega\} =$$
$$([\mathbf{E}]\,[\mathbf{P}]^{-1}[\mathbf{Q}] + [\mathbf{F}])\{\bar{e}_\Gamma\} + [\mathbf{E}][\mathbf{P}]^{-1}\{a\} + \{k\} . \qquad (8)$$

Equation (8) is solved as a time dependent problem. In the standard finite element method and finite difference method, first derivatives are calculated from differences of internal values. A rough discretization of the model often becomes a source of error even though internal values are obtained accurately. Since the IEM formulation is based on the BEM formulation, first derivatives in the α direction are obtained directly with high accuracy [11]:

$$\frac{\partial T}{\partial \alpha} = -\int_\Gamma T\frac{\partial}{\partial \alpha}\frac{\partial \phi^*}{\partial n}d\Gamma + \int_\Gamma \frac{\partial \phi^*}{\partial \alpha}\frac{\partial T}{\partial n}d\Gamma - \int_\Omega \frac{\partial \phi^*}{\partial \alpha}$$
$$\bullet\, \mu_0\sigma(\dot{T} + \frac{1}{4\pi}\mathbf{n}\bullet\int \dot{T}\frac{\partial}{\partial n}\frac{1}{R}dS)d\Omega - \int_\Omega \frac{\partial \phi^*}{\partial \alpha}\sigma\mathbf{n}\bullet\dot{\mathbf{B}}_0\, d\Omega . \qquad (9)$$

In an analysis of a branch structure in Fig. 1, a condition $T_1=T_2+T_3$ is obtained from Kirchhoff's current law ($J_1=J_2+J_3$) and (2), and the condition is imposed on T by the penalty number method [9]. In the analysis of a model with a hole in Fig. 2, total flux penetrating a hole is considered by two numerical techniques to solve a multiply connected problem [9]. One method is that the conductivity of the hole is assumed to be very small, where the hole region is also discretized as shown in Fig.2(a). The other method is that the hole is considered a patch element and T on the edge of the hole (•) in Fig.2(b) is constrained constant by the penalty number method. There is no discretization on the hole region in the second method.

NUMERICAL RESULTS AND DISCUSSION

Fig. 3 shows a filament current model of superconducting magnets of the levitation vehicle [1, 2]. When the velocity **V** of the rigid magnets is constant in the x direction, the applied magnetic field in (1) is expressed by the following velocity term :

$$\dot{\mathbf{B}}_0 = -\nabla\times(\mathbf{V}\times\mathbf{B}_0) = (\mathbf{V}\bullet\nabla)\mathbf{B}_0 = V_x\frac{\partial}{\partial x}\mathbf{B}_0 . \qquad (10)$$

The notation is also obtained from a different point of view [5] and a consideration of Lagrange derivative :

$$\dot{\mathbf{B}}_0 = \frac{\partial \mathbf{B}_0}{\partial t} = \frac{\partial x}{\partial t}\frac{\partial}{\partial x}\mathbf{B}_0 = V_x\frac{\partial}{\partial x}\mathbf{B}_0 . \qquad (11)$$

$$\frac{D\mathbf{B}_0}{Dt} = \frac{\partial \mathbf{B}_0}{\partial t} + (\mathbf{V}^*\bullet\nabla)\mathbf{B}_0 = \mathbf{0}\, ,\ \mathbf{V}^* = -\mathbf{V} . \qquad (12)$$

The same numerical solutions are obtained by using both source terms, i.e., the time derivative of the applied field in (1) and the velocity term of above equations.

A high manganese steel thin plate 10 cm × 10 cm × 3mm is placed on the same center line at a distance of 0.5 m, and the model is discretized to 16 × 16 elements. Its conductivity and relative permeability are $1.35\times10^6\ \Omega^{-1}m^{-1}$

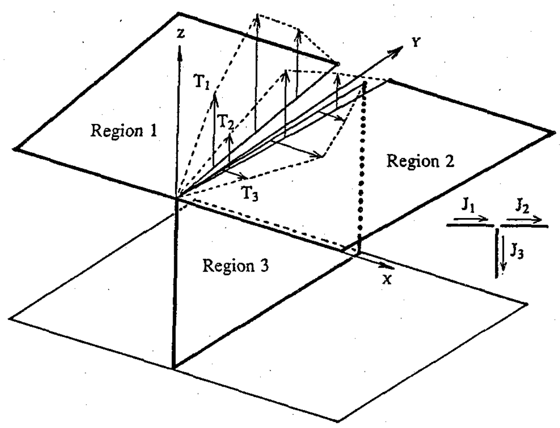

Fig.1 Branch structure and Kirchhoff's current law ($J_1=J_2+J_3$)

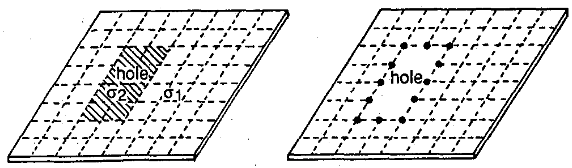

(a) Different conductivities (b) penalty number method

Fig.2 A plate with a hole

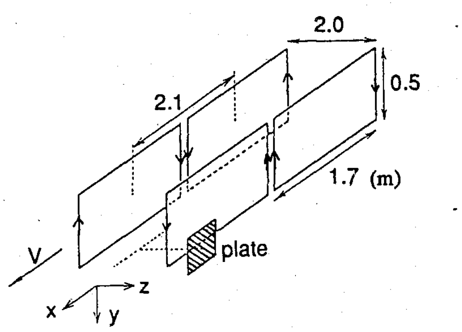

Fig.3 Numerical model of moving magnets

and 1.0, respectively. The velocity of magnets is assumed to be 200 km/h. When the plate is placed parallel to the moving magnets, applied magnetic field at a center of the plate, the total eddy current and the total Lorentz force are shown in Figs. 4,5. Solutions of a perpendicular plate are also shown in Fig. 6. Peaks of the eddy current and the Lorentz force coincide with those of time derivatives of the applied magnetic field. The total eddy current in a plate with a hole 3.75 cm × 7.5 cm is also shown in Fig. 4, where the same solution is obtained by using two methods in Fig.2. Figs.7 and 8 show total Lorentz force and eddy current distributions in the case of the right-angled plate and that of the L shaped plate of Fig. 9. The total Lorentz force of the L shaped plate is larger than the right-angled plate. These numerical results show that eddy current in a parallel part is dominant since the time derivative of B_z is larger than that of B_x. It is shown that eddy current flows into a vertical plate in the analysis of the H shaped plate of Fig.10.

CONCLUDING REMARKS

In the paper, Lorentz force acting on thin plates under the moving magnets is analyzed numerically by using the T-method and the IEM. Both methods have merits which are useful to the present analysis. Some numerical techniques are applied to the analysis of a branch structure and a multiply connected problem. Total eddy current and total Lorentz force are obtained for several simple thin plate structures. Further analyses of practical three dimensional structures will be carried out by using the two methods.

REFERENCES

[1] S.Fujiwara, "Characteristics of EDS magnetic levitation having ground coils for levitation arranged on the side wall", *Trans. IEE Japan*, vol. D-108, 439-446, 1988, (in Japanese).

[2] A.Yamashita, "Electromagnetic phenomena on guideway structures of magnetic levitation", in *Applied electromagnetics in materials*, K.Miya ed., Pergamon Press, pp.191-195,1989.

[3] I.Bolder and S.A.Nasar, *Linear motion electro-magnetic systems*, John Wiley & Sons, 1985

[4] F.C.Moon, *Magneto-solid mechanics*, John Wiley & Sons, 1985

[5] T.Takahashi and K.Kurita, "Computation of eddy currents induced in a conducting sheet under moving magnets", *IEEE Trans. Magn.*, vol.24, pp.197-200, 1988.

[6] D.Rodger, T.Karaguler and P.J.Leonard, " A formulation for 3D moving conductor eddy current problems", *IEEE Trans. Magn.*, vol.25, pp.4147-4149, 1989.

[7] K.Miya T.Sugiura and H.Hashizume, "Three dimensional analysis of an eddy current by the T-method", in *Electromagnetomechanical interaction in deformable solid and structures*, Y.Yamamoto and K.Miya ed., North Holland, pp.183-189,1987.

[8] K.Miya and H.Hashizume, "Application of T-method to AC problem based on BEM", *IEEE Trans. Magn.*, vol.24, pp.134-137, 1988.

[9] M.Tsuchimoto, M.Fukaya, M.Hashimoto, H.Hashizume, K.Miya and M.Seki, "Numerical and experimental eddy current analyses of complex first wall components of a fusion reactor", *Fusion Eng. Des*, in press.

[10] N.Tosaka and K.Kakuda, "An integral equation method for non-self-adjoint eigen value problems and its applications to non-conservative stability problems", *Int. J. Num. Meth. Eng.*, vol.20, pp.131-141, 1984.

[11] M.Tsuchimoto, A.Yoneta, T.Honma and K.Miya, "An analysis of the scalar helmholtz equation using the integral equation method", *IEEE Trans. Microwave Theory Tech.*, in press.

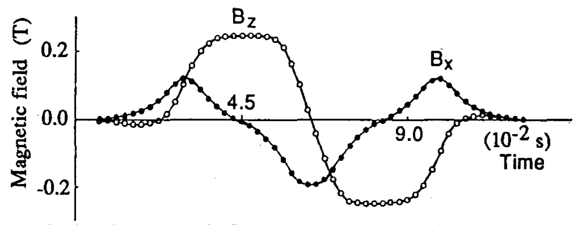

Fig.4 Applied magnetic field at a center of the plate produced by the passage of the magnets

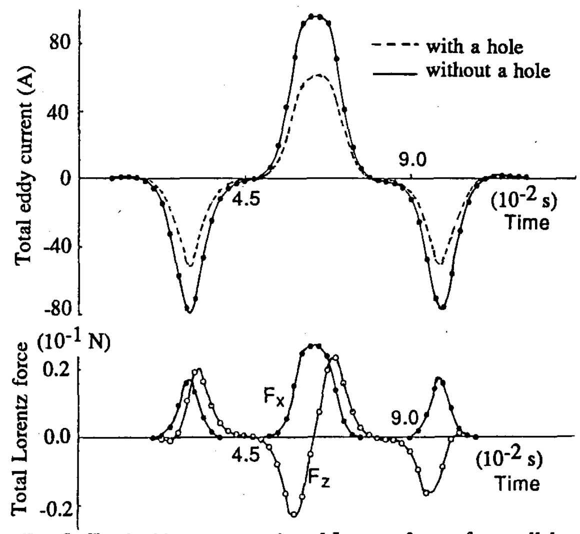

Fig.5 Total eddy current and total Lorentz force of a parallel plate

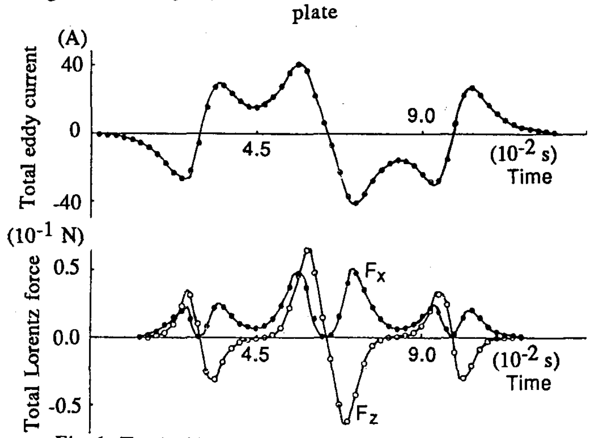

Fig.6 Total eddy current and total Lorentz force of a perpendicular plate

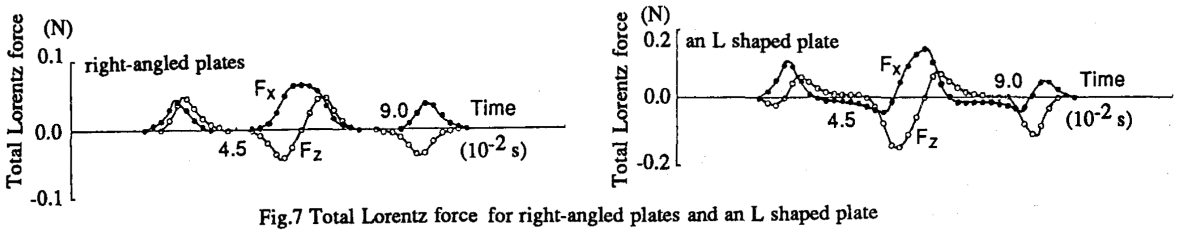

Fig.7 Total Lorentz force for right-angled plates and an L shaped plate

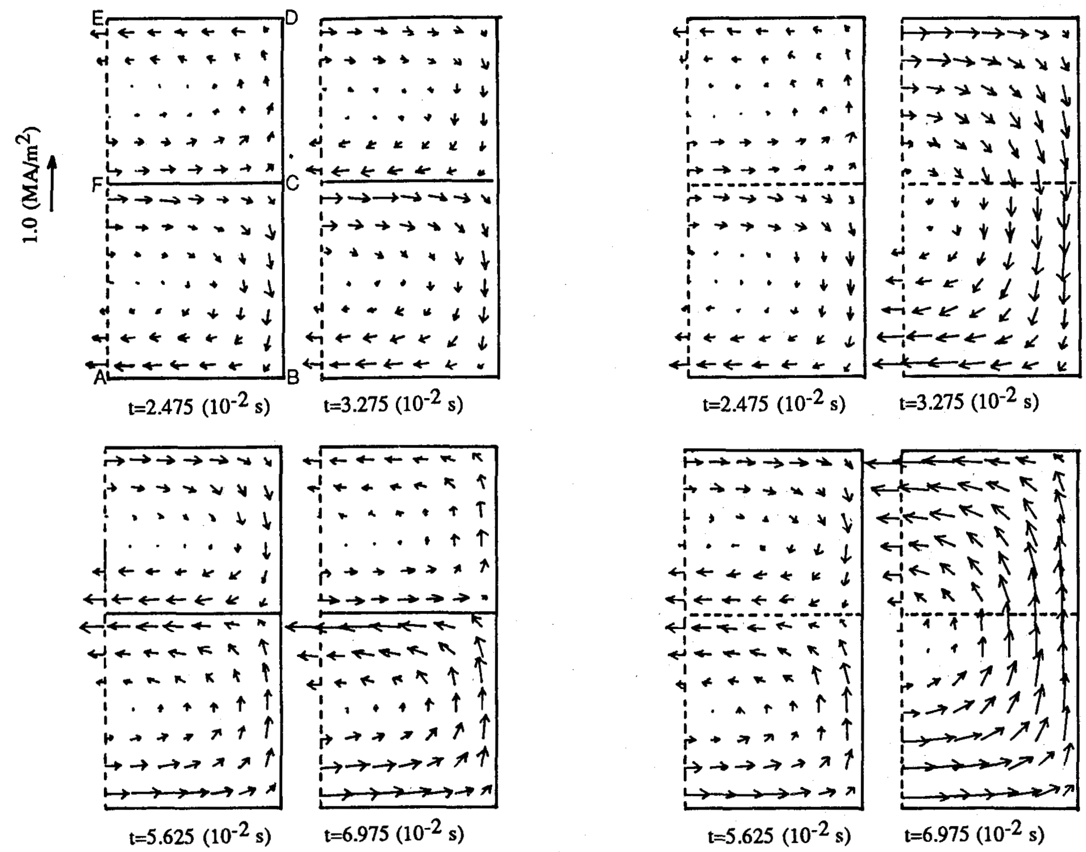

(a) right-angled two plates (b) an L shaped plate

Fig.8 Distributions of eddy current for right-angled plates and an L shaped plate

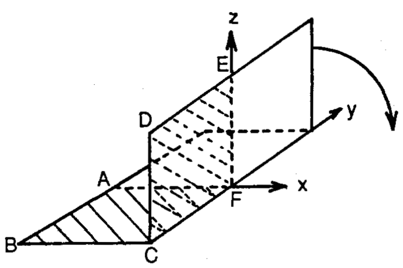

Fig.9 Numerical model of right-angled plates and an L shaped plate

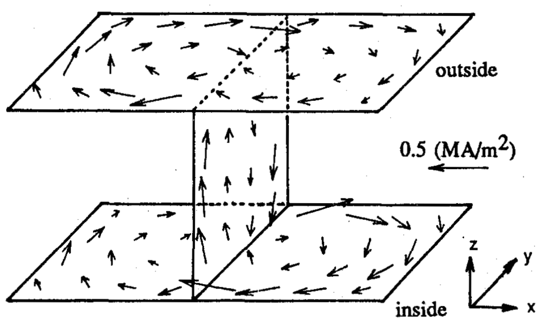

Fig.10 Distributions of eddy current for a H shaped plate at t=2.475 $(10^{-2}$ s)